6.8 A Pen-Pressure-Sensitive Capacitive Touch System Using Electrically Coupled Resonance Pen

Changbyung Park[1,2], Sungsoo Park[2], Ki-duk Kim[1], Sanghui Park[1], Juwan Park[2], Yunhee Huh[1], Byunghoon Kang[2], Gyu-hyeong Cho[1]

[1]KAIST, Daejeon, Korea, [2]Samsung Electronics, Suwon, Korea

Capacitive touch systems for finger touch have become widely used in mobile devices such as smartphones, tablets, and so on. Beyond ordinary touch functions, some devices adopt an extra electromagnetic resonance (EMR) system [1] to support pens for advanced user experiences; these devices have been successfully commercialized for high-end devices [2]. Such devices offer a realistic and accurate pen-based drawing experience for consumers using a battreryless, light, and pressure-sensitive pen; this is possible because the EMR system excites a passive pen via magnetic coupling and senses the pen's returning signal that contains coordinate and fine pen-pressure information. As shown in Fig. 6.8.1 (top), an EMR system, however, requires an additional costly sensor board made with a flexible printed circuit board beneath a display panel to find coordinates of the EMR pen via a magnetic field and a dedicated controller, and it also consumes excessive power. If a capacitive touch system could cover the function of the EMR system, it would be a cost-effective and compact solution in terms of re-utilizing an existing system without the additional sensor board and EMR controller. In this paper, a capacitive touch system sensing a passive pen with pen pressure as well as a finger is introduced as an alternative to an EMR system.

The sensing panel configuration and Electrically Coupled Resonance (ECR) pen are shown in Fig. 6.8.1. An ECR pen is composed of a conductive tip for electric coupling with the touch-screen panel (TSP) and LC resonant tank with pressure-to-capacitance transducer (P2CT) C_p and inductor L. To find touched points (TP) of the pen, a position sensor (PS) detects TP of both fingers and pen by means of constructing a touch image from the capacitance matrix of C_Ms. To sense pen pressure, C_p varies depending on applied pen pressure, thereby the resonant frequency f_r of the parallel resonant tank changes, i.e., f_r reflects the information of C_p (pen pressure). The f_r is converted to a corresponding pen pressure voltage V_{pp} by a pen pressure sensor (PPS).

Figure 6.8.2 (top) shows a multi TX scan (MTS) method. To sense a small C_M variation by a fine-tip pen with high SNR, a multiple driving scheme [4] based on a modified 8th Hadamard matrix $\boldsymbol{H}_8$ is used. The first and remaining columns of $\boldsymbol{H}_8$ are filled with 1s and balanced elements of 1s and -1s, respectively. Without a modification, the RX incoming charge corresponding with the first column is too large. Hence, in the modified $\boldsymbol{H}_8$, the first column is omitted and the remaining balanced columns are used; the RX incoming charge through static component (offset) of C_Ms is autonomously canceled out by the characteristic of the modified $\boldsymbol{H}_8$. Because only the dynamic component of C_M is sensed, an offset charge-canceling procedure [6] is not required. With the driving pattern based on the modified $\boldsymbol{H}_8$, there are 8 unknown mutual capacitances (C_{M0} ~ C_{M7}) in 7 equations; a touch image can be constructed using the relationship among C_Ms from the simultaneous equations. Since the MTS only finds the relationship among C_Ms in a group, there should be an overlapped TX electrode in adjacent groups to find the C_M relationship between the groups for the complete touch image.

Figure 6.8.2 (bottom) shows a charge-demodulating integrator (CDI) of PS. CDI has two sensing modes. One is an absolute sensing mode (ASM) that integrates the absolute amount of transferred charge from a single RX electrode to C_{int}, and the other is a differential sensing mode (DSM) that integrates the charge difference between adjacent channels to nullify common-mode display noise [3]. The two modes are convertible depending on control bit *diff*. For example, CDI normally operates in ASM, and it changes its operating mode to DSM, depending on the display noise environment. For both modes, in the demodulator, the RX incoming charges are stored in C_{d1} and C_{d3}, while the stored charges in C_{d2} and C_{d4} are transferred to the integrator at ϕ_{TX}=1, vice versa at ϕ_{TX}=0, where capacitances of $C_{d1\sim4}$ are the same. The charge-transferring polarity of each phase is opposite to demodulate charge. Since the positive charge and the negative charge with inverting operation are summed and integrated to C_{int}, low-frequency noise can be filtered [4]. In ASM, the charges in C_{d1}+C_{d3} and C_{d2}+C_{d4} are transferred to the integrator. In DSM, the difference between the charge in C_{d4} (C_{d3}) of the current channel and that of C_{d2} (C_{d1}) of the next channel is integrated to the integrator at ϕ_{TX}=1 (ϕ_{TX}=0) by cross coupling of C_{d4} (C_{d3}) and C_{d2} (C_{d1}); thereby, the differential sensing is concurrently done without input multiplexing.

Figure 6.8.3 shows the structure of the PPS and its timing chart. After PS finds TP, pen-pressure sensing is performed separately by PPS. Depending on the found TP, the nearest TX electrode to TP is driven, and the output of the amplifier U_1 in CDI that corresponds to TP is connected to PPS by a mux. In driving phase, a driven TX electrode excites the ECR pen with near-f_r, exploiting capacitive coupling, and resonant energy is charged in the ECR pen. In the sensing phase coming just after the stop of driving a TX electrode, the ECR pen still resonates with frequency f_r and the resonant voltage v_{st} at the tip of the ECR pen is sensed through C_{rs} and RX electrode, i.e., v_{st} is amplified to V_r by U_1 embedded at CDI. A comparator converts V_r to a digital signal ϕ_r. The reference frequency of f_r is set to 500kHz and PPS detects how much f_r is deviated from 500kHz (2µs period). A phase frequency detector (PFD) detects the phase difference between ϕ_r and 2µs-delayed ϕ_r (ϕ_{rd}) through a reference delay cell (RDC). To average and filter phase noise of ϕ_r, an integrator integrates the current pulses from a charge pump and V_{pp} is generated after the given number of integrations. PPS performs these driving-and-sensing pairs several times since it is hard to obtain enough noise performance and dynamic range at once due to the short resonant sustaining time in the ECR pen. Because the ECR pen can only resonate at a designated frequency, the system can detect the ECR pen on TSP by means of counting the number of pulses of ϕ_r. If the ECR pen is not detected, i.e., fingers are touched, PPS does not proceed to pen-pressure sensing.

The detailed structure of the delay calibrator with measurement waveforms is shown in Fig. 6.8.4. The RDC should be calibrated to guarantee the accuracy of PPS, because it is implemented using a current-starved inverter chain (CSIC) that is sensitive to PVT variations. Initializing the phase of PPS ϕ_{init} defines delay calibration phase in Fig. 6.8.3. During this phase, a reference frequency of 500kHz is applied to the TX electrode and resonance in ECR pen starts, and RDC is calibrated using this frequency at the same time. As long as the phase difference between the input TX_{ref} and TX_{refd} (delayed TX_{ref}) becomes zero, RDC has a propagation delay of the period of the reference, 2µs. The propagation delay of CSIC is inversely proportional to its bias current I_b, which is corrected by a calibration loop similar to a PLL. I_1 supplies the minimum operable current of RDC. The calibration loop corrects I_{cal} so that the phase difference becomes zero. After the calibration, V_{cal} is held at loop-compensation capacitor C_c and then PPS senses f_r of ECR pen with the calibrated RDC. Since PFD and a charge pump in the calibrator are not additionally required but shared with building blocks in PPS, it is much less complex than other schemes like digital calibrators.

Figure 6.8.5 (top) shows measurement results on a 10.1" commercial device. Waveforms of multi TX driving patterns based on the modified $\boldsymbol{H}_8$, the output voltages of PS V_ps for touched and untouched conditions with 6mm ϕ metal pillar are shown. A read-out touch image shows touched positions where 3 types of ϕ metal pillars of 1 and 2mm as a pen, and 6mm as a finger are touched on the TSP. Measured SNRs for 1mm ϕ, and 6mm ϕ metal pillars are 49 and 62dB, respectively. Measurements of PPS are shown in Fig. 6.8.5 (bottom), where the f_r of the ECR pen is lower than reference frequency of 500kHz in the transient waveform. Measured V_{pp} spread proves 6b accuracy of PPS on 6σ criteria. The monotonicity of pen-pressure voltage V_{pp} versus ΔC_p is verified by measurements, where the ΔC_p is the variation of C_p from the reference value that makes f_r 500kHz. From this curve, the host can calculate the applied pen pressure on the ECR pen. Performance is summarized in Fig. 6.8.6. The chip micrograph is shown in Fig. 6.8.7.

References:

[1] Wacom. EMR Technology [Online].
Available: http://www.wacom-components.com/english/technology/emr.html

[2] Samsung. Galaxy note3+Gear [Online].
Available: http://www.samsung.com/global/microsite/galaxynote3-gear/

[3] H. Shin, *et al.*, "A 55dB SNR with 240Hz Frame Scan Rate Mutual Capacitor 30×24 Touch-Screen Panel Read-Out IC Using Code-Division Multiple Sensing Technique," *ISSCC Dig. Tech. Papers*, pp. 388-389, Feb. 2013.

[4] J. Yang, *et al.*, "A Highly Noise-Immune Touch Controller Using Filtered-Delta-Integration and a Charge-Interpolation Technique for 10.1-inch Capacitive Touch-Screen Panels," *ISSCC Dig. Tech. Papers*, pp. 390-391, Feb. 2013.

[5] N. Miura, *et al.*, "1mm-Pitch 80×80-Channel 322Hz-Frame-Rate Touch Sensor with Two-Step Dual-Mode Capacitance Scan," *ISSCC Dig. Tech. Papers*, pp. 216-217, Feb. 2014.

[6] H. Jang, *et al.*, "2D Coded-Aperture-Based Ultra-Compact Capacitive Touch-Screen Controller with 40 Reconfigurable Channels," *ISSCC Dig. Tech. Papers*, pp. 218-219, Feb. 2014.

 978-1-4799-6224-2/15/$31.00 ©2015 IEEE

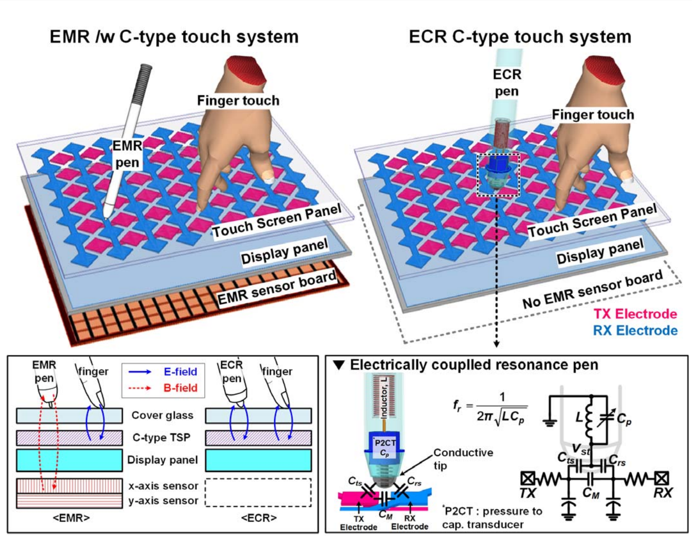

Figure 6.8.1: Overall configuration of the ECR touch system.

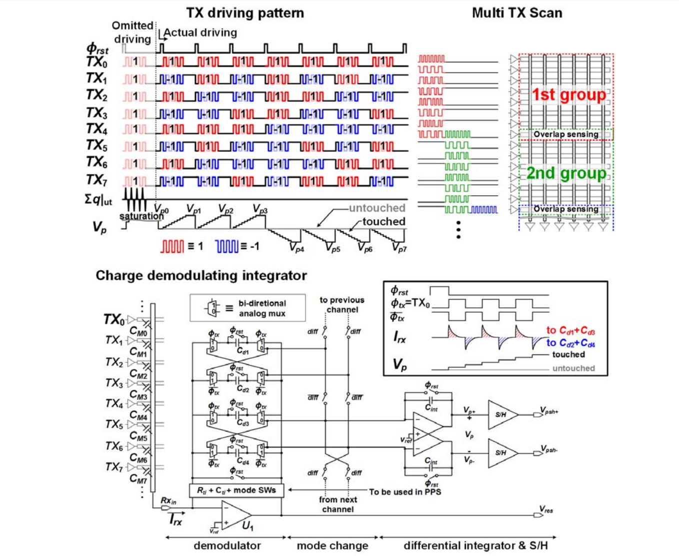

Figure 6.8.2: TX driving pattern, MTS, and the circuit implementation of CDI.

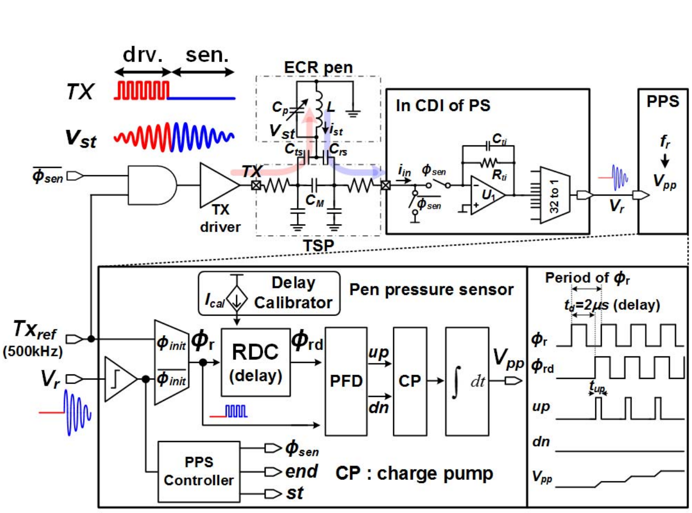

Figure 6.8.3: Implementation of pen-pressure sensor with its timing chart.

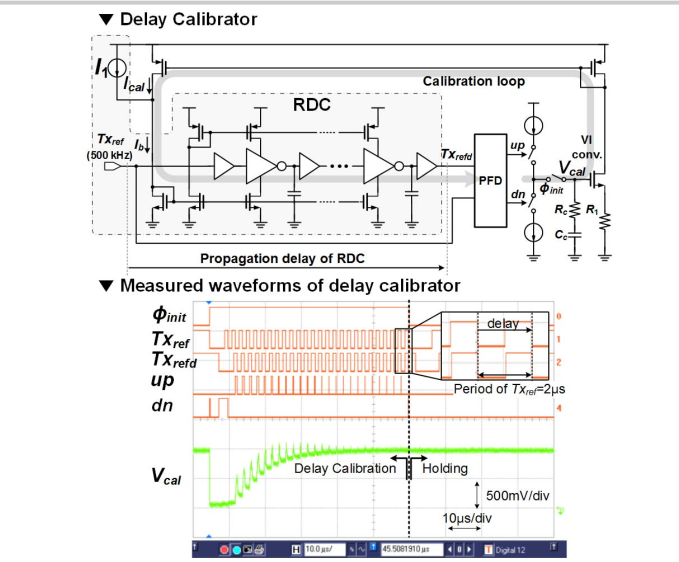

Figure 6.8.4: RDC delay calibrator and its measured waveforms.

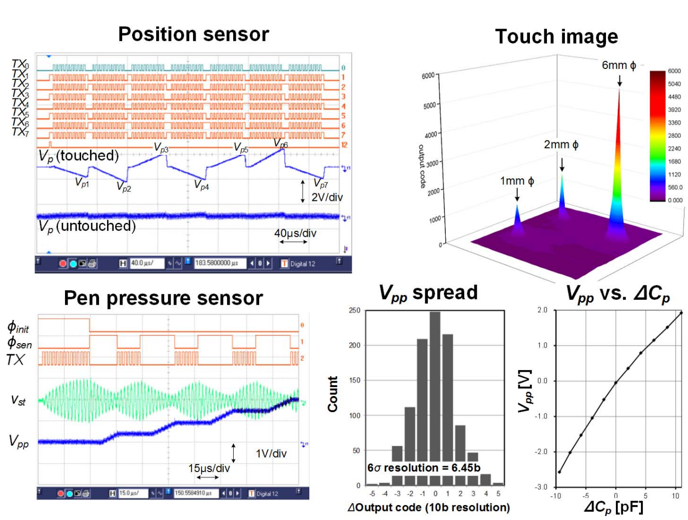

Figure 6.8.5: Measurement results.

	ISSCC 2013 [3]	ISSCC 2013 [4]	ISSCC 2014 [5]	ISSCC 2014 [6]	This work
Process	180nm CMOS	350nm CMOS	350nm CMOS	180nm CMOS	180nm BCD
Pen pressure	N/A	N/A	N/A	N/A	**Support (6 bit)**
TSP Size	5"	10.1"	4.5"	4.8"	10.1"
TSP type	Mutual	Mutual	Mutual	Mutual	Mutual
# of channels	TX : 30 RX : 24	TX : 27 RX : 43	TX:80 RX:80	TX : 24 RX : 16	TX : 48 RX : 32
Scan rate	240Hz	120Hz	322Hz	160Hz	120Hz
SNR	1mmϕ 35dB; finger 55dB	39dB (finger)	1mmϕ 32dB; finger 41dB	53 dB (finger)	1mmϕ **49 dB**; 6mmϕ **62 dB**
Power	52.8mW	18.7mW	21.8mW	2.6mW	30mW
Chip area	14.9mm²	10.4mm²	6.25mm²	0.46 mm² (Active)	14.7mm²

Figure 6.8.6: Performance summary

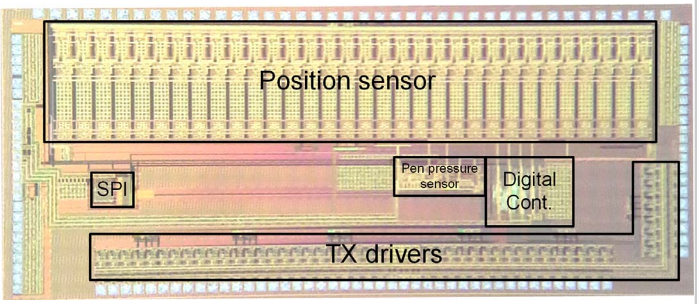

Figure 6.8.7: Chip micrograph.